Nanoscale

Accepted Manuscript

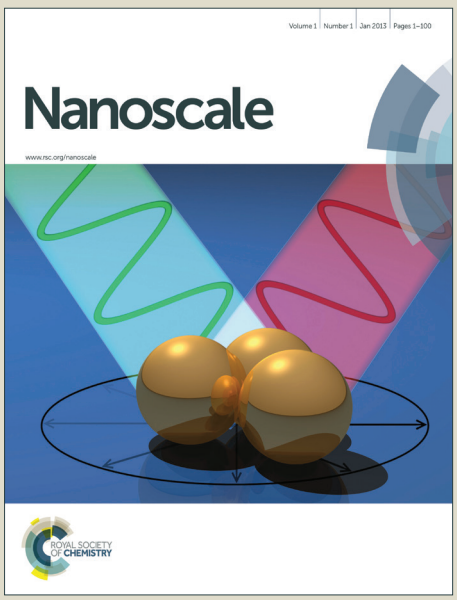

ROYAL SOCIETY OF CHEMISTRY

www.rsc.org/nanoscale

Cite this: DOI: 10.1039/c0xx00000x

www.rsc.org/xxxxxx

ARTICLE TYPE

Large-volume hot spots in gold spiky nanoparticle dimers for high-performance surface-enhanced spectroscopies†

Anran Li,[a] Shuzhou Li *[a]

Received (in XXX, XXX) Xth XXXXXXXXX 20XX, Accepted Xth XXXXXXXXX 20XX

DOI: 10.1039/b000000x

Hot spots with large electric field enhancement usually come with small volumes, limiting their applications in surface-enhanced spectroscopies. Using finite-difference time-domain method, we demonstrate that spiky nanoparticle dimer (SNPD) can provide hot spots with both large electric field enhancement and large volume because of the pronounced lightning rod effect of spiky nanoparticle. We find that the strongest electric fields lie in the gap region when SNPD is in a tip-to-tip (T-T) configuration. The enhancement of electric fields ($|E|^2/|E_0|^2$) in T-T SNPD with a 2 nm gap can be as large as $1.21x10^6$. And the hot spots volume in T-T SNPD is almost 7 times and 5 times larger than that in spike dimer and sphere dimer with the same gap size of 2 nm, respectively. Hot spots volume in SNPD can be further improved by manipulating the arrangements of spiky nanoparticles, where crossed T-T SNPD provides the largest hot spots volume being 1.5 times of that in T-T SNPD. Our results provide a strategy to obtain hot spots with both intense electric fields and large volume by adding a bulky core at one end of the spindly building block in dimers.

Introduction

In the past, noble metal nanoparticles have been extensively studied for highly sensitive surface-enhanced spectroscopies, for example, surface-enhanced Raman scattering (SERS), surface-enhanced fluorescence and surface-enhanced infrared absorption.[1-4] SERS has significant advantages in chemical and biological sensing because of its ultrahigh sensitivity and specificity in combination with remarkable signal enhancement.[5, 6] According to earlier studies, SERS is the result of chemical enhancement and the electromagnetic (EM) enhancement, where EM enhancement is thought to play a dominant role.[5, 7-9] When the enhancement of emission light is similar to that of incident light, the EM enhancement factor scales roughly as the fourth power of local electric field magnitude ($|E|^4/|E_0|^4$).[5, 8, 10] Metallic nanoparticles (NPs) have received intense interests as SERS substrates due to their ability to produce intensified electric fields stemming from the excitation of localized surface plasmon resonance (LSPR).[1, 6, 11-13] For good SERS substrates, high sensitivity, reproducibility, and reliability are required.[14-17] Generally, amplifying electric field enhancement is important for high sensitive SERS detection, and increasing "hot spots volume" is essential for reproducible and reliable SERS detection.[14-18]

Nanostructures with anisotropic shapes have been demonstrated to produce intense electric fields localized at their sharp features.[19-21] For example, hot spots can be generated at the sharp corners of the nanoplates in silver nano-flags.[19] In high-density branched silver nanowires, hot spots can be produced and localized at the corners, branches, and knobs.[21] Nevertheless, the electric field enhancement in single NP is relative small. Compared with single NP, NP dimers can generate much larger electric fields and have been extensively explored as effective substrates to generate a greatly enhanced Raman signal.[2, 10, 18, 22-24] Single-molecule detections have also been demonstrated by using NP dimers.[24-27] Upon aggregation, NPs can couple with adjacent ones through near field interaction, producing hot spots regions with intensely enhanced electric fields localized at the nanoscale junctions. For instance, extremely enhanced electric fields can be generated and confined at the interparticle junctions in adjacent nanoplates due to the plasmon coupling effect.[28] These hot spots in adjacent nanoplates are significant for biochemical sensing, optical processing, and solar photovoltaic applications.[28] It has been proven that the incident polarization, gap spacing, particle shape and relative arrangement all significantly affect the plasmonic properties of dimers.[2, 18, 29-34] In previous studies, two types of hot spots are of interest: hot spot with the largest electric field enhancement which is important for single-molecule SERS, and hot spot with large volume which can support the greatest average electric field enhancement and promote the reproducible and reliable SERS detection.[18, 31] Nevertheless, hot spots in dimers are usually with small volumes, increasing the challenge of directing analytes into nanoscale hot spots. One strategy to optimize hot spots in metallic NPs is by masking their cold spots and exposing only the hot spots regions.[35, 36] The improved SERS performance is due to the decreased cold areas, allowing molecules to bind only at hot spots regions. However, the actual "hot spots volume" in these studies is still small. Another strategy to increase the "hot spots volume" in NP dimers is to increase the coupling surface by manipulating the arrangements of nanoparticles.[18, 22] For example, nanocube

dimer with face-to-face configuration can provide hot spots with much larger volumes than that in nanocube dimer with edge-to-edge configuration.[29, 30] Compared with pyramidal nanoshell dimers with side-to-side arrangement, 4-fold increase of the Raman signal in pyramidal nanoshell dimers with stacked configuration can be observed resulting from the 4-fold increase of the number of parallel surfaces.[37] However, increasing coupling surface in NP dimer reduces the small curvature of the geometry at the coupling areas, resulting in weaker "lightning rod effect" and therefore smaller electric field enhancement.

In this paper, we demonstrate that dimers composed of spiky nanoparticles (SNPs) can provide hot spots with both large maximum electric field enhancement and large volumes, overcoming the limitation that large-volume hot spots usually come with a sacrifice of maximum electric field enhancement. SNP is composed by a bulky core with protruding sharp tips and has been extensively explored for SERS, LSPR refractive index sensing, diagnostics, and photothermal therapy because of its extremely enhanced electric fields localized at sharp tips.[38-48] According to previous studies of Nordlander and coworkers, the plasmon resonance of SNP could be viewed as the hybridization of plasmons of the central spherical core and rodlike spikes, corresponding to the bonding and anti-bonding resonance modes, respectively.[20] In SNP, the spike enabled the focalization of electric fields at its apex due to "lightning rod effect".[20, 49] In addition, the spherical core of SNP could serve as an electron reservoir and a nanoscale antenna, noticeably enhancing local electric fields of the spike plasmons compared to that of isolated spike.[20, 49]

In this study, SNP composed by a bulky spherical core and a single spike is selected as the building block of dimers. The near-field and far-field properties of spiky nanoparticle dimers (SNPDs) with different configurations are investigated using 3D finite-difference time-domain (FDTD) method.[50] Akin to previous study about nanocube dimer, we firstly investigate the optical properties of SNPD with tip-to-tip (T-T), tip-to-sphere (T-S) and sphere-to-sphere (S-S) configurations, which are analogous to nanocube dimers with edge-to-edge, edge-to-face and face-to-face arrangements, respectively. We find that T-T SNPD exhibits the largest electric field enhancement ($|E|^2/|E_0|^2$) with a value as high as 1.21×10^6 when the gap is 2 nm. This value is much higher than that in general dimer structures (usually with a value of $\sim 10^4$). In addition, T-T SNPD exhibits ~7 times and ~5 times larger “hot spots volume” than that in spike dimer and sphere dimer with the same 2 nm gap, respectively. More importantly, we demonstrate that crossed T-T SNPDs can provide further increased “hot spots volume” which is almost 2 times of that in T-T SNPD. Our results indicate that SNPD can provide hot spots with both large maximum electric field enhancement and volume, breaking the general limitation that large-volume hot spot usually comes with a small maximum electric field enhancement. Inspired by the large-volume hot spots in SNPDs, we propose a strategy to obtain hot spots with both intense electric fields and large volume in dimers by adding a bulky core at one end of the spindly building blocks.

Numerical method

The optical properties of SNPDs are modeled by 3D FDTD method.[50] For all simulations, a total-field scattered-field plane wave source is selected to estimate the interaction between propagating plane wave and gold nanostructures. Vacuum is taken as external medium. The dielectric function of gold is obtained from a generalized multi-coefficient model[51] that fits the dispersion data obtained from Johnson and Cristy.[52] To get accurate results, override mesh regions are used for each part of the nanostructure. Specifically, a mesh size as small as 0.25 nm is used at the gap regions of dimers and a mesh size of 1 nm is used in other regions. Before all simulations, convergence testing is carefully done to verify the accuracy and stability of the calculations. Here, all calculations are performed using a commercial simulation program (FDTD solutions 7.5, Lumerical solutions, Inc., Vancouver, Canada).

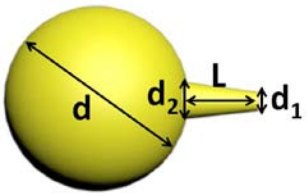

Fig. 1 Schematic illustration of a single spiky nanoparticle. The spike is represented by a truncated cone with the tip diameter (d_1) of 10 nm, bottom diameter (d_2) of 22.5 nm and spike length (L) of 50 nm. The spherical core refers to a diameter (d) of 50 nm.

In this study, all the dimers are with at least 2 nm separations. The gap with 2 nm or larger size enables the adsorption of large molecules at the gap junction, which is essential for the investigation of large biomolecules. Fig. 1 shows the schematic geometry of single SNP constructed in FDTD simulations. The SNP is represented by a spherical core with a protruding surface spike. The spike is represented by a truncated cone with the tip diameter (d_1) of 10 nm, bottom diameter (d_2) of 22.5 nm and spike length (L) of 50 nm. The spherical core in all calculations refers to a diameter (d) of 100 nm. The size parameters of SNP are selected according to previous studies by Pedireddy et al. and Chini’s research group.[53, 54]

Results and discussion

The schematic illustrations of S-S, T-S and T-T SNPDs are depicted in the inset of Fig. 2(a). The wave vector ($\vec{k}$) and polarization direction ($\vec{E}$) of incidence are indicated by the blue arrow and red arrow, respectively. Fig**.** 2**(**a**)** shows the extinction spectra of S-S, T-S and T-T SNPDs with fixed gap size of 2 nm. The dotted line represents the extinction spectrum of single SNP. As expected, "interparticle coupling" can generate noteworthy red-shift of the resonance peak.[55] In addition, T-T SNPD can generate the largest red shift of resonance peak upon coupling, followed by T-S SNPD and then S-S SNPD. Despite the low-energy resonance modes with large extinction cross sections, there are also other resonance peaks appearing in the extinction spectrum of each dimer. Calculated electric field distributions (Fig**.** S1†) indicate that resonance mode at 617 nm in S-S SNPD is dominated by the coupled plasmon resonance at the gap region. The resonance modes at 526 nm and 805 nm in T-S SNPD are corresponding to the modes dominated by sphere plasmon

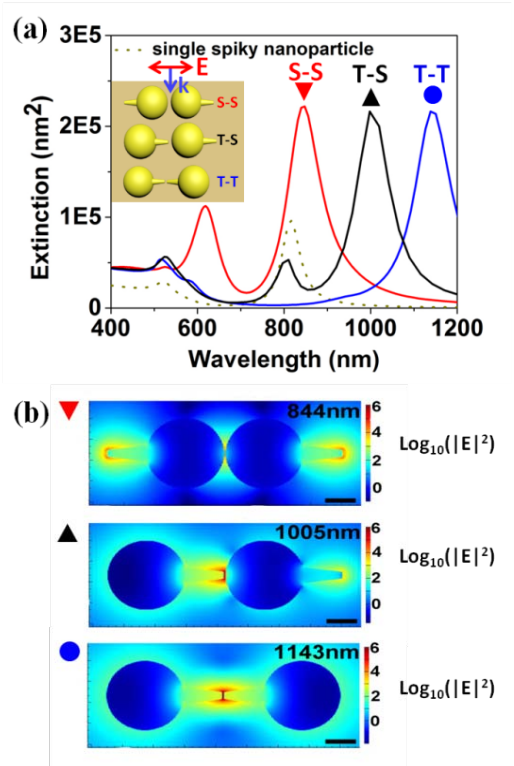

Fig. 2 (a) Extinction spectra for sphere-to-sphere (S-S), tip-to-sphere (T-S) and tip-to-tip (T-T) spiky nanoparticle dimers (SNPDs). The gap in all dimers is 2 nm. The dotted line represents the extinction spectrum for single spiky nanoparticle (SNP). (b) Electric field distributions ($\log_{10}(|E|^2/|E_0|^2)$) for three dimers at their resonant wavelengths, which are labeled by inverted triangle, triangle and solid circles in (a). The scale bar in each figure is 50 nm.

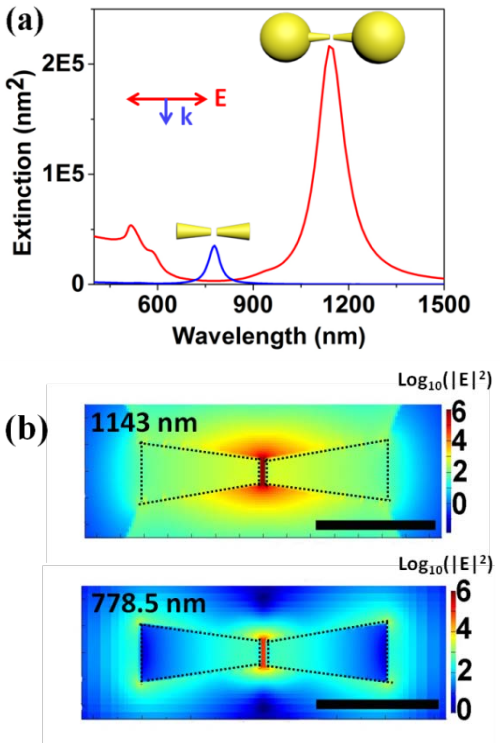

Fig. 3 (a) Extinction spectra of spike dimer and tip-to-tip spiky nanoparticle dimer. The gap distances in all calculations are 2 nm. (b) Electric field distributions ($\log_{10}(|E|^2/|E_0|^2)$) at the resonant peak with the lowest energy for each dimer. The scale bar in each figure is 50 nm. The dashed black lines in (b) show the outlines of spikes.

resonance and spike plasmon resonance, respectively. And the resonance mode at 515 nm in T-T SNPD is corresponding to the mode dominated by sphere plasmon resonance.

Fig. 2(b) shows the electric field distribution for each dimer at their corresponding low-energy resonant peaks, i.e., the peaks labeled by inverted triangle, triangle and solid circles in Fig. 2(a). The planes of the electric field maps are both selected to parallel to the incidence polarization direction and bisect the center of the SNPD. Strong electric fields located at both gap region and spikes can be observed at the resonant wavelength of 844 nm in S-S SNPD. At the resonant wavelength of 1005 nm for T-S SNPD, electric fields are mainly distributed at the T-S gap regions and the spike plasmon resonance is weakly excited. For T-T SNPD, electric fields are confined at the T-T gap region at the resonant wavelength of 1143 nm, indicating that the resonance mode at 1143 nm is attributed to the coupling mode at T-T gaps. According to the calculations, T-T SNPD with 2 nm gap size exhibits the largest electric field enhancement ($|E|^2/|E_0|^2$) with a value of $1.21\text{x}10^6$. This value is much higher than that in general dimer structures (usually with a value of ~10^4) with the same gap size.

The larger resonance position shift and higher electric field enhancement in T-T SNPD can be ascribed to the best synergistic interaction of "interparticle coupling" and "lightning rod effect" in T-T SNPD. Due to "lightning rod effect", more charges will be distributed at the spike tip. In T-T SNPD, the spike tip happens to be at the interparticle junction, promoting the near-field coupling at the T-T junction. Whereas, the "lightning rod effect" will attract more charges away from the S-S gap junctions in S-S SNPD, resulting in weak "interparticle coupling" strength. The peak wavelength and electric field enhancement for S-S, T-S and T-T SNPDs with various gap sizes are shown in electronic supplementary information (Fig. S2†). Followed by dipolar-coupling model[56], the calculated resonance position and electric field enhancement for all SNPDs versus gap sizes are well fitted using single exponential equations. The exponential fitting parameters are listed in detail in electronic supplementary information (Table S1 and S2†).

Besides the extremely enhanced electric fields, SNPDs can also provide hot spots with extremely large volume. Fig. 3 shows the comparison between T-T SNPD and spike dimer. Here, spike dimer is composed of two spikes without the spherical core, as shown in the inset of Fig. 3(a). The gap size for both dimers is 2 nm. With the addition of bulky spherical core at the bottom of the spike, both increased extinction intensity and pronounced red shift of the resonance peak can be observed. At the same time, adding spherical cores can significantly enhance the electric fields at the spike to spike gap regions (Fig. 3(b)). According to the calculations, the maximum electric field enhancement ($|E|^2/|E_0|^2$) in T-T SNPD is $1.21\text{x}10^6$. This value is about 15 times of that in spike dimer whose maximum electric field enhancement is $8.18\text{x}10^4$. More importantly, the electric fields in

Table 1. Calculated "hot spots volumes" for various nanostructures under their resonant conditions.

nanostructure	resonant wavelength (nm)	"hot spots volume" (nm^3)	
		$\|E\|^2/\|E_0\|^2>10^4$	$\|E\|^2/\|E_0\|^2>10^5$
single spike	645.5	0	0
spike dimer	778.5	335.5	0
sphere dimer	633.5	493.5	0
T-T SNPD	1143	2301	349
T-S SNPD	1005	2608	349
S-S SNPD	844	1127	0

T-T SNPD are more delocalized along the sharp spikes comparing with spike dimer without spherical cores, indicating a much larger "hot spots volume". The extremely enhanced electric fields in T-T SNPD are associated with the "lightning rod effect" of sharp spike.[20, 41, 57] For one thing, the spherical core can serve as an electron reservoir. For another thing, the spike tends to be sharper with the appearance of spherical core, attracting more charges to the spike side. Moreover, the strong "interparticle coupling" at the junction between two spikes of T-T SNPD also helps to pump up charges into the gap junction. The cooperative interaction of these three factors results in extremely enhanced electric fields localized at gap region for T-T SNPD. Figure 3 suggest that simultaneously increased electric field enhancement and hot spots volume can be obtained in NP dimers by adding a bulky core at one end of the building blocks.

Table 1 shows the calculated "hot spots volumes" for spike dimer, sphere dimer and SNPDs under their corresponding resonant conditions. Gap separations for all dimers are fixed at 2 nm. We first define regions with electric field enhancement ($|E|^2/|E_0|^2$) larger than $1x10^4$ as hot spots. And "hot spots volume" is defined as the total volumes of all the regions with electric field enhancement larger than $1x10^4$. With this definition, "hot spots volume" in T-T SNPD is 7 times and 5 times larger than that in spike dimer and sphere dimer, respectively, due to the pronounced synergistic effect of "lightning rod effect" of spiky geometry and "interparticle coupling" of dimer structure. The "hot spots volume" in T-S SNPD is slightly larger than that in T-T SNPD, and S-S SNPD produces the smallest "hot spots volume". When defining the "hot spots volume" as the total volumes of all the regions with electric field enhancement larger than $1x10^5$, both T-T SNPD and T-S SNPDs exhibits "hot spots volume" of 349 nm^3. The "hot spots volume" for both spike dimer and sphere dimer is 0. According to previous studies, large-volume hot spots usually come with the sacrifice of the maximum electric field enhancement.[29, 30] Nevertheless, Table 1 quantitatively demonstrates that SNPD can provide hot spots with both large maximum electric field enhancement and large volume, indicating the great potentials of SNPDs in surface-enhanced spectroscopies, such as SERS.

Moreover, we show that hot spots in SNPDs can be further improved by manipulating the arrangement of SNPs into crossed tip-to-tip configuration. Schematic illustration of crossed T-T SNPD is shown in the inset of Fig. 4(a). The parallel distance between two spikes is fixed at 2 nm and x represents the overlap

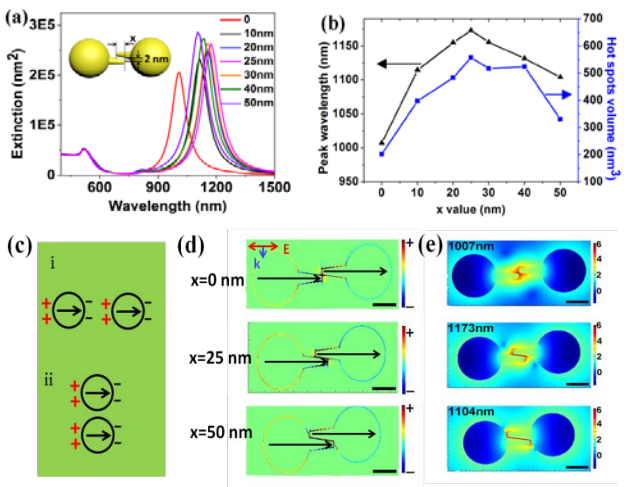

Fig. 4 (a) Extinction spectra of the crossed tip-to-tip (T-T) spiky nanoparticle dimers (SNPDs) with various x values ranging from 0 to 50 nm. The inset shows the schematic illustration of a crossed T-T SNPD. (b) The shift of the red most resonance peak (left y-axis) and calculated "hot spots volumes" (right y-axis) for crossed T-T SNPDs as a function of x values. The hot spots are defined as regions with electric field enhancement ($|E|^2/|E_0|^2$) larger than 10^5. (c) Schematic illustration of dipole-dipole interaction model. The black arrows represent the dipole moment. (d) Charge distributions of crossed T-T SNPDs with x value of 0 nm, 25 nm and 50 nm under their corresponding resonant conditions. (e) Electric field distributions ($\log_{10}(|E|^2/|E_0|^2)$) of crossed T-T SNPDs at x values of 0 nm, 25 nm and 50 nm under their corresponding resonance conditions. The scale bar in each figure is 50 nm.

distance between two spikes. The results indicate the resonance peak shows a volcano shift trend with increasing overlap x, i.e., the resonance peak red shifts firstly with increasing x, and then blue shifts with further increasing x (Fig. 4(a) and (b)). The turning point is at x~25 nm. This volcano shift trend can be explained through a simple dipole-dipole interaction model.[58] Fig. 4(c) shows two typical dipole-dipole interactions. For (i), the attractive force between negative charge of the left particle and positive charge of the right particle weakens the repulsive forces within each particle, resulting in the decrease of the resonance frequency and therefore the red shift of the resonance peak. And the resonance position shows red shift with decreasing interparticle separation. For (ii), the attractive force between positive (negative) charge of the upper particle and negative (positive) charge of the lower particle can enhance the repulsive action in both particles, leading to the blue shift of resonance position. In this case, the resonance position blue shifts with decreasing interparticle spacing. In crossed T-T SNPDs with x smaller than 25 nm, the charge distribution at resonant wavelength approaches to the charge distribution in (i) (Fig. 4(d), x=0 nm). Therefore, dipole-dipole interaction (i) plays a dominant role. In this case, increasing x is equivalent to decreasing the interparticle separation, resulting in the red shift of resonance position. For crossed T-T SNPDs with x larger than 25 nm, the dipole-dipole interaction (ii) plays a key role. With increasing x, the charge distribution in crossed T-T approaches to the charge distribution in (ii) (Fig. 4(d), x=50 nm). Hence, the resonance position blue shift with increasing x.

Table 2. Calculated "hot spots volumes" for crossed T-T SNPDs with different overlap x values under their corresponding resonant conditions.

Crossed T-T SNPD	resonant wavelength (nm)	"hot spots volume" (nm^3)	
		$\|E\|^2/\|E_0\|^2>10^4$	$\|E\|^2/\|E_0\|^2>10^5$
x=0	1007	3388.5	201.5
x=10	1114.5	3310	397.5
x=20	1155	3297	483
x=25	1173	3324	557.5
x=30	1155.5	3196	517
x=40	1131.5	3271.5	523.5
x=50	1104	3600.5	330

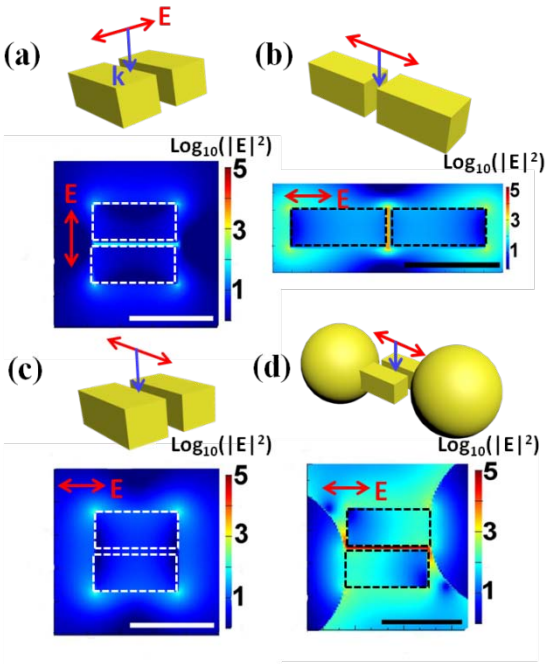

Fig. 5 Influence of bulky spherical core on the electric field enhancement in cuboid dimers. (a, c) Electric field distributions of parallel aligned cuboid dimers with different polarized incidence. (b) Electric field distribution of longitudinally aligned cuboid dimer. (d) Electric field distribution of parallel aligned cuboid dimer after adding bulky spherical cores at one end of each cuboid. All calculations are performed at their corresponding resonant conditions. The dashed line in each figure is the outline of cuboid structure. The scale bar in each figure is 50 nm.

Fig. 4(e) shows the electric field distributions for crossed T-T SNPDs with x values of 0 nm, 25 nm and 50 nm at their corresponding resonant wavelengths. The electric fields for each dimer are mainly distributed at the junction between two parallel spikes, resulting from the intense coupling between the positive charge at one spike and the negative charge at another spike. It has been demonstrated in previous research that electric fields are extremely decreased in side-by-side assembly of gold nanorods.[59] However, Fig. 4(e) show that the maximum electric field enhancement ($|E|^2/|E_0|^2$) in crossed T-T SNPDs can always be

Table 3. Calculated "hot spots volumes" for crossed T-T SNPDs with different spherical core sizes ranging from 50 nm to 400 nm under their corresponding resonant conditions.

Crossed T-T SNPD (x=25 nm)	resonant wavelength (nm)	"hot spots volume" (nm^3)	
		$\|E\|^2/\|E_0\|^2>10^4$	$\|E\|^2/\|E_0\|^2>10^5$
d=50	980	1509	166.5
d=100	1173	3324	557.5
d=200	1343	5864	834.5
d=300	1468	5469	773.5
d=400	1675	3721	501

larger than 10^5 when manipulating x from 0 to 50 nm. The intense electric fields localized at the junction between two parallel spikes in crossed T-T SNPD are believed to stem from the addition of bulky spherical core at the end of spikes. With the appearance of the bulky core, more charges will be attracted to the spike side because of the prominent "lightning rod effect", resulting in intense "interparticle coupling" and therefore large electric fields localized at the spike-to-spike junction.

Ascribing to the large coupling area between long spikes, crossed T-T SNPDs is anticipated to provide further increased "hot spots volume". Fig. 4(b) and Table 2 show the calculated "hot spots volumes" for crossed T-T SNPDs with various overlap distances. When defining "hot spots volume" as the whole volumes of all regions with electric field enhancement larger than $1x10^4$, "hot spots volume" in crossed T-T SNPDs is always ~1.5 times of that in T-T SNPDs, regardless of the overlap distance x. When the "hot spots volume" is calculated as the whole volumes of all regions with electric field enhancement larger than $1x10^5$, "hot spots volume" in crossed T-T SNPDs can also be 1.5 times of that in T-T SNPD by manipulating x values.

Inspired by the large-volume hot spots in crossed T-T SNPD, we propose a strategy to obtain hot spots with both large maximum electric field enhancement and large volume in dimers by adding a bulky core at one end of the spindly building blocks. With the addition of a bulky structure at one end of the spindly structure, more charges will be attracted to the spindly structure due to "lightning rod effect", resulting in large electric field enhancement within interparticle junction. To further demonstrate this theory, we performed simulations on cuboid dimers (Fig.5). The length, width, and height of gold cuboid are 50 nm, 25 nm, and 25 nm, respectively. And the edges of the cuboid are rounded with a radius of 2 nm. The gap distance for all dimers is 2nm. Extinction spectra of all dimers in Fig. 5 are shown in electronic supplementary information (Fig. S3†). Electric field distributions for all dimers are calculated at their corresponding resonant conditions. Fig. 5 shows clearly that electric field enhancement in cuboid dimers with face-to-face configuration is always small, regardless of the relative arrangement of NP and polarization direction of incidence. For longitudinally aligned cuboid dimer shown in Fig. 5 (b), the largest electric field enhancement within gap is $7.15x10^3$. For parallel aligned cuboid dimer shown in Fig. 5 (c), electric fields are mainly focused at the sharp corners of cuboid structure where a maximum electric field enhancement of 1521 is obtained. Nevertheless, after introducing a bulky sphere at one end of each cuboid in parallel aligned cuboid dimer, the

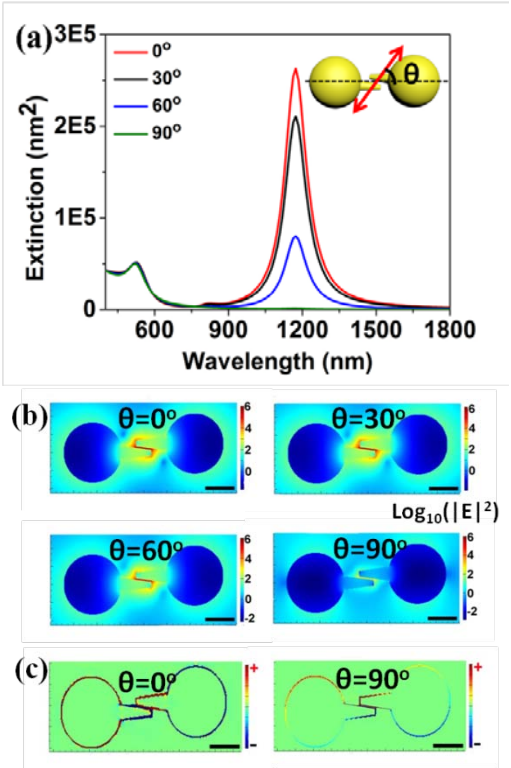

Fig. 6 Influence of incidence polarization on the optical property of crossed tip-to-tip (T-T) spiky nanoparticle dimer (SNPD) with 25 nm overlap. (a) Calculated extinction spectra of crossed T-T SNPD with θ ranging from 0°to 90°. (b) Electric field distribution ($\log_{10}(|E|^2/|E_0|^2)$) in crossed T-T SNPD for different incidence polarization. (c) Charge distributions of crossed T-T SNPD for θ=0°and θ=90°. The scale bar in each figure is 50 nm.

largest electric field enhancement at the gap region is extremely enhanced to a value as high as $7.33x10^4$ (Fig. 5(d)). More importantly, hot spots with volume as large as 2893 nm^3 can be achieved in cuboid dimer with bulky core under its resonant conditions, where hot spots is defined as the whole volumes of all regions with electric field enhancement larger than $1x10^4$.

Aforementioned results indicate that bulky core plays a significant role in optimizing the electric field enhancement and "hot spots volume" in SNPDs. Table 3 shows the influence of the spherical core size on the "hot spots volume" of crossed T-T SNPDs. And the maximum electric field enhancements in crossed T-T SNPDs with various spherical sizes are shown in Table S3. When increasing spherical core diameter from 50 nm to 200 nm, both the maximum electric field enhancement and the "hot spots volume" show great increase. This can be ascribed to the increased "lightning rod effect". With increasing spherical core size, the spike tends to be relative sharper, resulting in more pronounced "lightning rod effect". In addition, being an electron reservoir, larger spherical core is able to provide more electrons to be attracted to the spike side, generating stronger electric field enhancement.[20] Nevertheless, the role of spike becomes weaker when the sphere core is large enough. Further increasing spherical core size from 200 nm to 400 nm, gradually decreased maximum electric field enhancement and "hot spots volume" in crossed T-T SNPDs are observed. The extinction spectra of crossed T-T SNPD with different spherical diameters are shown in electronic supplementary information (Fig. S4†). The resonance peak with lowest energy red shift with increasing spherical size. Moreover, the resonance peak gradually broadened with increasing sphere core diameter due to increased radiative damping. An extremely broadened resonance peak is observed for SNPD with 400 nm spherical core.

Finally, we demonstrate that hot spots in SNPDs depend strongly on the incident polarization. As shown in Fig. 6(a), the polarization direction of incidence has no influence on the resonance position but only leads to the change of the intensity of resonance peak. With increasing θ, the intensity of resonance peak located at 1173 nm decreases gradually. When θ equals to 90°, the peak located at 1173 nm cannot be observed any more. The influence of polarization direction in the intensity of resonance peak is consistent with the phenomenon that has been observed in previous study about single SNP.[20] Fig. 6(b) shows the calculated electric field distribution for crossed T-T SNPD under differently polarized incidence. The results indicate that the electric field enhancement decreases with increasing θ. The maximum electric field enhancement is obviously decreased to 10^3 when θ equals to 90°. This is because when θ equals to 90°, spike mode in individual SNP cannot be efficiently excited (Fig. 6(c)). Hence, the electric fields cannot be effectively confined at spike tip, resulting in pronounced decrease of the electric field enhancement in the gap of crossed T-T SNPD.

Conclusions

In summary, the present study provides a strategy to obtain hot spots with both large maximum electric field enhancement and large volume, overcoming the general limitation that large-volume hot spot usually comes with a sacrifice of the maximum electric field enhancement. We show that T-T SNPD with 2 nm gap size exhibits the largest electric field enhancement ($|E|^2/|E_0|^2$) with a value as high as $1.21x10^6$. In addition, T-T SNPD exhibits ~7 times and ~5 times larger "hot spots volume" than that in spike dimer and sphere dimer, respectively. In addition, the "hot spots volume" in SNPD can be optimized by manipulating the arrangement of SNPs, where crossed T-T SNPD exhibits the largest "hot spots volume", followed by T-S SNPD, then T-T SNPD, and finally S-S SNPD. The simultaneously increased electric field enhancement and "hot spots volume" in SNPD is ascribed to the pronounced synergetic effect of "interparticle coupling" and "lightning rod effect". Recent research indicated that electric fields at the spike region rapidly increase with increasing spike length.[53] Therefore, even higher electric field enhancement can be obtained in crossed T-T SNPD through fabricating SNP with longer spikes. At the same time, SNP with longer spike can further increase the potential "hot spots volume". Also note that the resonant position of SNPDs is located at the near-infrared regions, which is significant for in vivo biological sensing due to the high transparency of tissue in near-infrared regions. Inspired by the large-volume hot spots in SNPDs, we propose that hot spots with both large maximum electric field enhancement and large volume can be generated by adding a bulky core at one end of the spindly building block in dimers. We hope our results can provide guidelines in optimizing metallic nanostructures for surface-enhanced spectroscopies.

Acknowledgements

S.L. and A.L. thank the support by the Singapore NRF under the CREAT program of Nanomaterials for Energy and Water Management and the support from MOE Tier 2 (ACR12/12). S.L. also thanks the support from A*Star (SERC 112-120-2011).

Notes and references

[a] *School of Materials Science and Engineering , Nanyang Technological University, Singapore 639798. Email: lisz@ntu.edu.sg;*

† Electronic Supplementary Information (ESI) available. See DOI: 10.1039/b000000x/

1. M. Rycenga, C. M. Cobley, J. Zeng, W. Li, C. H. Moran, Q. Zhang, D. Qin and Y. Xia, *Chem. Rev.*, 2011, **111**, 3669-3712.
2. N. J. Halas, S. Lal, W. S. Chang, S. Link and P. Nordlander, *Chem. Rev.*, 2011, **111**, 3913-3961.
3. H. Chen, L. Shao, Q. Li and J. Wang, *Chem. Soc. Rev.*, 2013, **42**, 2679-2724.
4. L. Jiang, Y. Sun, F. Huo, H. Zhang, L. Qin, S. Li and X. Chen, *Nanoscale*, 2012, **4**, 66-75.
5. A. Campion and P. Kambhampati, *Chem. Soc. Rev.*, 1998, **27**, 241-250.
6. J. N. Anker, W. P. Hall, O. Lyandres, N. C. Shah, J. Zhao and R. P. Van Duyne, *Nat. Mater.*, 2008, **7**, 442-453.
7. G. C. Schatz, *Acc. Chem. Res.*, 1984, **17**, 370-376.
8. M. Moskovits, *Rev. Mod. Phys.*, 1985, **57**, 783-826.
9. K. Kneipp, H. Kneipp, I. Itzkan, R. R. Dasari and M. S. Feld, *Chem. Rev.*, 1999, **99**, 2957-2975.
10. J. M. McMahon, S. Li, L. K. Ausman and G. C. Schatz, *J. Phys. Chem. C*, 2011, **116**, 1627-1637.
11. K. M. Mayer and J. H. Hafner, *Chem. Rev.*, 2011, **111**, 3828-3857.
12. P. L. Stiles, J. A. Dieringer, N. C. Shah and R. P. Van Duyne, *Ann. Rev. Anal. Chem.*, 2008, **1**, 601-626.
13. H. Zhu, H. Chen, J. Wang and Q. Li, *Nanoscale*, 2013, **5**, 3742-3746.
14. G. Lu, H. Li, S. Wu, P. Chen and H. Zhang, *Nanoscale*, 2012, **4**, 860-863.
15. K. Qian, H. Liu, L. Yang and J. Liu, *Nanoscale*, 2012, **4**, 6449-6454.
16. Y. Yang, Z.-Y. Li, K. Yamaguchi, M. Tanemura, Z. Huang, D. Jiang, Y. Chen, F. Zhou and M. Nogami, *Nanoscale*, 2012, **4**, 2663-2669.
17. Z. Liu, Z. Yang, B. Peng, C. Cao, C. Zhang, H. You, Q. Xiong, Z. Li and J. Fang, *Adv. Mater.*, 2014, **26**, 2431-2439.
18. K. A. Stoerzinger, J. Y. Lin and T. W. Odom, *Chem. Sci.*, 2011, **2**, 1435-1439.
19. X.-Y. Zhang, T. Zhang, A. Hu, Y.-J. Song and W. W. Duley, *Appl. Phys. Lett.*, 2012, **101**, 153118.
20. F. Hao, C. L. Nehl, J. H. Hafner and P. Nordlander, *Nano Lett.*, 2007, **7**, 729-732.
21. X. Y. Zhang, T. Zhang, S. Q. Zhu, L. D. Wang, X. Liu, Q. L. Wang and Y. J. Song, *Nanoscale Res. Lett.*, 2012, **7**.
22. H. Wei and H. Xu, *Nanoscale*, 2013, **5**, 10794-10805.
23. J. Fischer, N. Vogel, R. Mohammadi, H. J. Butt, K. Landfester, C. K. Weiss and M. Kreiter, *Nanoscale*, 2011, **3**, 4788-4797.
24. K. L. Wustholz, A. I. Henry, J. M. McMahon, R. G. Freeman, N. Valley, M. E. Piotti, M. J. Natan, G. C. Schatz and R. P. V. Duyne, *J. Am. Chem. Soc.*, 2010, **132**, 10903-10910.
25. J. P. Camden, J. A. Dieringer, Y. Wang, D. J. Masiello, L. D. Marks, G. C. Schatz and R. P. Van Duyne, *J. Am. Chem. Soc.*, 2008, **130**, 12616-12617.
26. A. M. Michaels, J. Jiang and L. Brus, *J. Phys. Chem. B*, 2000, **104**, 11965-11971.
27. S. Nie and S. R. Emory, *Science*, 1997, **275**, 1102-1106.
28. X.-Y. Zhang, A. Hu, T. Zhang, W. Lei, X.-J. Xue, Y. Zhou and W. W. Duley, *ACS Nano*, 2011, **5**, 9082-9092.
29. P. H. C. Camargo, L. Au, M. Rycenga, W. Li and Y. Xia, *Chem. Phys. Lett.*, 2010, **484**, 304-308.
30. B. Gao, G. Arya and A. R. Tao, *Nat. Nanotechnol.*, 2012, **7**, 433-437.
31. E. Hao and G. C. Schatz, *J. Chem. Phys.*, 2004, **120**, 357-366.
32. J. M. Romo-Herrera, R. A. Alvarez-Puebla and L. M. Liz-Marzán, *Nanoscale*, 2011, **3**, 1304-1315.
33. L. Shao, C. Fang, H. Chen, Y. C. Man, J. Wang and H.-Q. Lin, *Nano Lett.*, 2012, **12**, 1424-1430.
34. K. C. Woo, L. Shao, H. Chen, Y. Liang, J. Wang and H. Q. Lin, *ACS Nano*, 2011, **5**, 5976-5986.
35. E. D. Diebold, P. Peng and E. Mazur, *J. Am. Chem. Soc.*, 2009, **131**, 16356-16357.
36. M. Rycenga, M. R. Langille, M. L. Personick, T. Ozel and C. A. Mirkin, *Nano Lett.*, 2012, **12**, 6218-6222.
37. K. A. Stoerzinger, W. Hasan, J. Y. Lin, A. Robles and T. W. Odom, *J. Phys. Chem. Lett.*, 2010, **1**, 1046-1050.
38. L. Rodríguez-Lorenzo, R. A. Álvarez-Puebla, F. J. G. De Abajo and L. M. Liz-Marzán, *J. Phys. Chem. C*, 2010, **114**, 7336-7340.
39. Y. Pei, Z. Wang, S. Zong and Y. Cui, *J. Mater. Chem. B*, 2013, **1**, 3992-3998.
40. W. Ma, M. Sun, L. Xu, L. Wang, H. Kuang and C. Xu, *Chem. Commun.*, 2013, **49**, 4989-4991.
41. H. Yuan, Y. Liu, A. M. Fales, Y. L. Li, J. Liu and T. Vo-Dinh, *Anal. Chem.*, 2013, **85**, 208-212.
42. S. K. Dondapati, T. K. Sau, C. Hrelescu, T. A. Klar, F. D. Stefani and J. Feldmann, *ACS Nano*, 2010, **4**, 6318-6322.
43. L.-C. Cheng, J.-H. Huang, H. M. Chen, T.-C. Lai, K.-Y. Yang, R.-S. Liu, M. Hsiao, C.-H. Chen, L.-J. Her and D. P. Tsai, *J. Mater. Chem.*, 2012, **22**, 2244-2253.
44. C. G. Khoury and T. Vo-Dinh, *J. Phys. Chem. C*, 2008, **112**, 18849-18859.
45. L. Osinkina, T. Lohmüller, F. Jäckel and J. Feldmann, *J. Phys. Chem. C*, 2013, **117**, 22198-22202.
46. A. M. Fales, H. Yuan and T. Vo-Dinh, *J. Phys. Chem. C*, 2014, **118**, 3708-3715.
47. D. H. M. Dam, K. S. B. Culver and T. W. Odom, *Mol. Pharmaceutics*, 2014, **11**, 580-587.
48. J. Lee, B. Hua, S. Park, M. Ha, Y. Lee, Z. Fan and H. Ko, *Nanoscale*, 2014, **6**, 616-623.
49. L. Shao, A. S. Susha, L. S. Cheung, T. K. Sau, A. L. Rogach and J. Wang, *Langmuir*, 2012, **28**, 8979-8984.
50. A. Taflove and S. C. Hagness, *Computational electrodynamics : the finite-difference time-domain method*, Boston : Artech House, c2005. 3rd ed., 2005.
51. http://www.lumerical.com.
52. P. B. Johnson and R. W. Christy, *Phys. Rev. B*, 1972, **6**, 4370-4379.
53. S. Pedireddy, A. Li, M. Bosman, I. Y. Phang, S. Li and X. Y. Ling, *J. Phys. Chem. C*, 2013, **117**, 16640-16649.

54. D. Pabitra, K. Abhitosh, K. Pandian Senthil, L. Nicolas and C. Tapas Kumar, *Nanotechnology*, 2013, **24**, 405704.
55. K. H. Su, Q. H. Wei, X. Zhang, J. J. Mock, D. R. Smith and S. Schultz, *Nano Lett.*, 2003, **3**, 1087-1090.
56. P. K. Jain, W. Huang and M. A. El-Sayed, *Nano Lett.*, 2007, **7**, 2080-2088.
57. Y. Hsiangkuo, G. K. Christopher, H. Hanjun, M. W. Christy, A. G. Gerald and V.-D. Tuan, *Nanotechnology*, 2012, **23**, 075102.
58. W. Rechberger, A. Hohenau, A. Leitner, J. R. Krenn, B. Lamprecht and F. R. Aussenegg, *Opt. Commun.*, 2003, **220**, 137-141.
59. A. Lee, A. Ahmed, D. P. dos Santos, N. Coombs, J. I. Park, R. Gordon, A. G. Brolo and E. Kumacheva, *J. Phys. Chem. C*, 2012, **116**, 5538-5545.